International Journal of Cardiology 249 (2017) 461–466

Contents lists available at ScienceDirect

International Journal of Cardiology

journal homepage: www.elsevier.com/locate/ijcard

A novel method for evaluating regional RV function in the adult congenital heart with low-dose CT and SQUEEZ processing

Francisco J. Contijoch [a,b], Daniel W. Groves [c], Zhennong Chen [a], Marcus Y. Chen [c], Elliot R. McVeigh [a,b,d,*]

[a] Department of Bioengineering, UC San Diego, La Jolla, CA, United States
[b] Department of Radiology, UC San Diego, La Jolla, CA, United States
[c] Cardiovascular and Pulmonary Branch, Division of Intramural Research, National Heart, Lung, and Blood Institute, National Institutes of Health, Bethesda, MD, United States
[d] Division of Cardiology, Department of Medicine, UC San Diego, La Jolla, CA, United States

ARTICLE INFO

Article history:
Received 9 June 2017
Received in revised form 17 July 2017
Accepted 14 August 2017
Available online 29 September 2017

Keywords:
Adult congenital heart disease
Cardiac computed tomography
Systolic function

ABSTRACT

Background: Measuring local RV function in adult congenital heart disease (ACHD) with echocardiography or MRI is challenging because of the complex geometry and existing pacing devices. Visual assessment of ventricular function via low-dose cardiac CT has been recently performed. This pilot study assessed whether low-dose 4D cine CT combined with automatic measurement of regional shortening could quantify right-ventricular function in ACHD patients.
Methods: Seven patients with Tetralogy of Fallot either contraindicated for MRI or assessed for coronary artery disease and seven non-congenital patients were imaged with ECG-gated cardiac CT utilizing a 320-detector row scanner. Right ventricular global function and regional shortening were quantified.
Results: Non-congenital patients were imaged with 2.9 ± 2.1 mSv and 395 ± 359 HU blood-myocardium contrast. The ACHD patients were imaged with 2.1 ± 1.3 mSv and 726 ± 296 HU contrast. Right ventricles of the ACHD patients had higher end-diastolic volume (297 ± 107 mL vs 123 ± 34 mL, $p = 0.001$), lower ejection fraction (32.0 ± 4.9% vs 45.0 ± 6.0%, $p = 0.001$), and higher dyskinetic fraction (10.9 ± 3.7% vs 2.6 ± 2.8%, $p < 0.001$) relative to the non-congenital controls.
Conclusions: In this initial pilot study, right ventricular global and regional systolic function were measured using low-dose cine CT with SQUEEZ quantification in non-congenital patients as well as ACHD patients with Tetralogy of Fallot. Unique regional features of RV dyskinesia were identified in the ACHD patients which could yield a more precise quantification of RV function.

1. Introduction

Adults with congenital heart disease (ACHD) represent a growing portion of adult cardiovascular care [1]. As these patients enter adulthood, there is a clinical need for routine assessment of cardiac function to identify the onset of ventricular dysfunction, tailor medical therapy, and recommend interventions such as valve replacement or cardiac resynchronization therapy [2].

Assessment of ventricular function in ACHD patients with echocardiography is challenging due to the complex anatomy, often large ventricle sizes, and poor echocardiographic windows after surgery [3]. Cardiac magnetic resonance imaging (MRI) has been the gold-standard as a non-ionizing imaging method to provide accurate volumetric information. However, cardiac MRI may be contraindicated in patients with pacemakers or implantable cardioverter-defibrillators [3].

Traditionally, cardiac computed tomography (CT) has been limited by the radiation exposure and limited temporal resolution when compared to echocardiography and cardiac MRI [3]. However, a low radiation dose, contrast-enhanced, retrospectively-gated cardiac CT protocol with a median radiation dose of <1 mSv was recently shown to successfully evaluate global biventricular systolic function in 30 consecutive patients [4]. Furthermore, quantification of regional shortening via 4D cine CT using SQUEEZ [5] analysis has recently been shown to distinguish normal and infarcted regions of the left ventricle and has been validated using MRI tagging [5,6].

In this pilot study, we combine these two advances in CT imaging to demonstrate the ability of low radiation dose retrospectively-gated CT combined with SQUEEZ processing to quantify the distribution of right ventricular regional shortening in normal adults as well as ACHD patients with Tetralogy of Fallot. This approach provides both global and

* Corresponding author at: Department of Bioengineering, University of California San Diego, 9500 Gilman Dr. MSC 0412, La Jolla, CA 92093-0412, United States.
E-mail address: emcveigh@ucsd.edu (E.R. McVeigh).

http://dx.doi.org/10.1016/j.ijcard.2017.08.040
0167-5273/

regional measures of systolic function that can be utilized to monitor function longitudinally as well as quantify response to treatment.

2. Methods

Patients were scanned under an IRB approved protocol at the National Institutes of Health. The study protocol conformed to the ethical guidelines of the 1975 Declaration of Helsinki. All subjects provided written informed consent to participate. The ACHD patients were at least 18 years old with congenital heart disease and were clinically referred for contrast-enhanced cardiac CT. Exclusion criteria were pregnancy or renal dysfunction, estimated glomerular filtration rate <30 mL/min/1.73 m^2 [7]. Patients were not excluded for weight, heart rate, or heart rhythm.

2.1. Patient population

Overall, 14 patients were included in the study. Relevant demographics are shown in Table 1. Seven patients without congenital heart disease were imaged due to concern of coronary artery disease and served as anatomical controls (#1–7). The imaging showed no or non-obstructive epicardial coronary artery disease and had sufficient myocardium-blood contrast (>170 HU) in the RV for SQUEEZ quantification of function. Seven ACHD patients with repaired Tetralogy of Fallot were included in the study (#8–14). The imaging and clinical condition of each patient are outlined below.

All congenital patients had a prior transannular patch repair.

Patient 8 had prior pulmonary valve replacement, and biventricular pacemaker implantation and was referred for biventricular assessment of systolic function.

Patient 9 was referred for biventricular assessment for evaluation of right-ventricular end-diastolic size and systolic function in consideration for pulmonary valve replacement. A breast tissue expander after mastectomy was a contraindication for MRI.

Patient 10 had prior pulmonary valve replacement, residual ventricular septal defect repair, and dual-chamber ICD implantation and was referred for biventricular assessment of systolic function.

Patient 11 had a re-do repair with reconstructed right ventricular outflow tract, recurrent VSD patch repair, and was referred for coronary artery and biventricular functional assessment.

Patient 12 was referred for coronary artery and biventricular functional assessment. The scan spanned two RR-intervals due to arrhythmia.

Patient 13 had a prior bioprosthetic pulmonary valve replacement and was referred for coronary artery and biventricular functional assessment.

Patient 14 had a prior percutaneous closure of an atrial septal defect, dual-chamber ICD placement, aortic aneurysm, and was referred for biventricular functional assessment.

2.2. Image acquisition

Patients underwent cardiac CT scans with axial imaging using a second-generation, 320 × 0.5-mm detector row CT unit (Aquilion ONE ViSION Edition; Toshiba Medical Systems, Otawara, Japan) with a gantry rotation time of 275 ms and acquisition over the entire cardiac cycle. End-diastolic and end-systolic frames for non-congenital and adult congenital patients are shown in Fig. 1A–B.

For the non-congenital patients as well as congenital patients referred for assessment of coronary arteries, a dose modulation protocol was performed to allow for assessment of the coronary arteries and systolic function. The maximum tube current is reported in Table 1. ACHD patients 8–10 and 14 underwent a low radiation dose retrospectively-gated cardiac CT scan to assess biventricular function. Patients 11–13 were referred for simultaneous function and coronary imaging and therefore received higher radiation dose imaging at end-diastole to visualize the coronary arteries.

Tube potential and tube current were determined by automatic exposure control (^{SURE}Exposure3D, Toshiba Medical Systems) on the basis of the X-ray attenuation on scout images and reconstruction kernel [8]. Images were reconstructed with a 512 × 512 matrix, 0.5 mm thick sections, and 0.25-mm increments using kernel FC03, iterative reconstruction AIDR3D in "standard" mode (Toshiba Medical Systems, Otawara, Japan).

Right ventricular (RV) blood-myocardium contrast was quantified via the difference in Hounsfield units between the myocardial blood pool and septal myocardium measured in axial images. Contrast-to-noise ratio (CNR) was estimated by dividing the contrast by the standard deviation of the intensity observed in the anterior chest wall.

2.3. Regional quantification of function

Regional shortening quantification was carried out using custom software in MATLAB. The basic steps were 1) short-axis reformatting of the 4-dimensional dataset, 2) ITK-SNAP region-growing segmentation of the RV blood volume at each timeframe, 3) calculation of RV volumes and ejection fraction, 4) SQUEEZ analysis [5] of 3D RV blood volumes with the "template" volume being the earliest timeframe after the QRS and the "target" volumes being the subsequent time points.

SQUEEZ analysis estimates the deformation of small triangular faces on the endocardial surface over time. For a patch v, the SQUEEZ value is:

$$\mathrm{SQUEEZ}(v,t) = \sqrt{\frac{A(v,t)}{A(v,0)}}$$

where t is the frame in the cine CT images and A is the area of the patch v. This yields a length measure of shortening. We report regional shortening from CT (RS_{CT}) as $RS_{CT} = (\mathrm{SQUEEZ} - 1)$.

Fig. 1C–E illustrates the how regional shortening is quantified. For visualization, the size of the triangles has been increased and three example triangles are shown depicting normal, hypokinetic, and dyskinetic motion. From the global volume curve, the minimum volume time frame is labeled end-systole and RS_{CT} values from this timeframe are obtained. Dyskinetic segments have end-systolic RS_{CT} values >0.

The heterogeneity of regional shortening was visualized by rendering end-systolic regional shortening values on the RV blood volume surface.

Dyskinesia was quantified via the percentage of the endocardial surface with end-systolic lengthening (RS_{CT} at end-systole >0). The mean and standard deviation of end-systolic RS_{CT} across the endocardial surface are reported in Table 2.

2.4. Statistical analysis

Differences in patient demographics, X-ray dose, image quality, and right ventricular function were evaluated via a two-way, unpaired, Student's *t*-test with a significance level of $p < 0.05$.

3. Results

3.1. Patient population

The ACHD patients were significantly ($p = 0.03$) taller (170.7 ± 7.5 cm) than the normal controls (159.6 ± 7.4 cm) but there were no significant differences in age ($p = 0.06$), weight ($p = 0.52$), or BMI ($p = 0.48$).

Table 1
Demographic patient information, radiation dose and RV enhancement for non-congenital patients (1–7) and ACHD patients (8–14). The average and standard deviation are shown beneath each group. CNR: contrast-to-noise ratio.

Patient	ACHD	Sex	Age	Height (cm)	Weight (kg)	BMI (kg/m^2)	Dose (mSv)	X-ray energy (kV)	Maximum tube current (mA)	RV blood-myocardium contrast (Hu)	CNR
1	N	F	59	163	58.2	22.0	1.22	100	250	690.3	21.2
2	N	M	47	173	97.7	32.8	6.13	100	790	174.2	4.4
3	N	F	52	163	88.6	33.5	0.75	80	140	1089.2	21.7
4	N	F	67	157	99.7	40.4	3.18	100	820	265.2	6.7
5	N	F	61	152	54.6	23.5	1.52	100	330	215.9	6.3
6	N	F	53	157	77.3	31.2	5.27	100	690	181.4	5.5
7	N	F	51	152	59.1	25.4	2.78	100	420	149.6	5.0
			55.7 ± 6.9	159.6 ± 7.4	76.4 ± 19.4	29.8 ± 6.5	3.0 ± 2.1	97.1 ± 7.6	491 ± 274	395.1 ± 358.9	10.1 ± 7.8
8	Y	M	33	174	84.0	27.7	3.24	80	220	710.8	14.5
9	Y	F	49	171	86.4	29.5	2.41	80	320	528.3	10.2
10	Y	F	48	170	63.2	21.8	0.60	80	90	1272.3	37.9
11	Y	M	45	175	109.1	35.5	3.38	100	240	358.3	9.0
12	Y	M	41	180	94.3	29.1	3.11	100	470	685.6	18.7
13	Y	F	43	156	66.4	27.3	1.07	80	450	608.9	12.9
14	Y	F	56	169	73.2	25.6	0.70	80	250	915.0	20.4
			45.0 ± 7.2	170.7 ± 7.5	82.4 ± 16.2	28.1 ± 4.2	2.1 ± 1.2	85.7 ± 9.8	291 ± 134	725.6 ± 295.5	17.7 ± 9.8

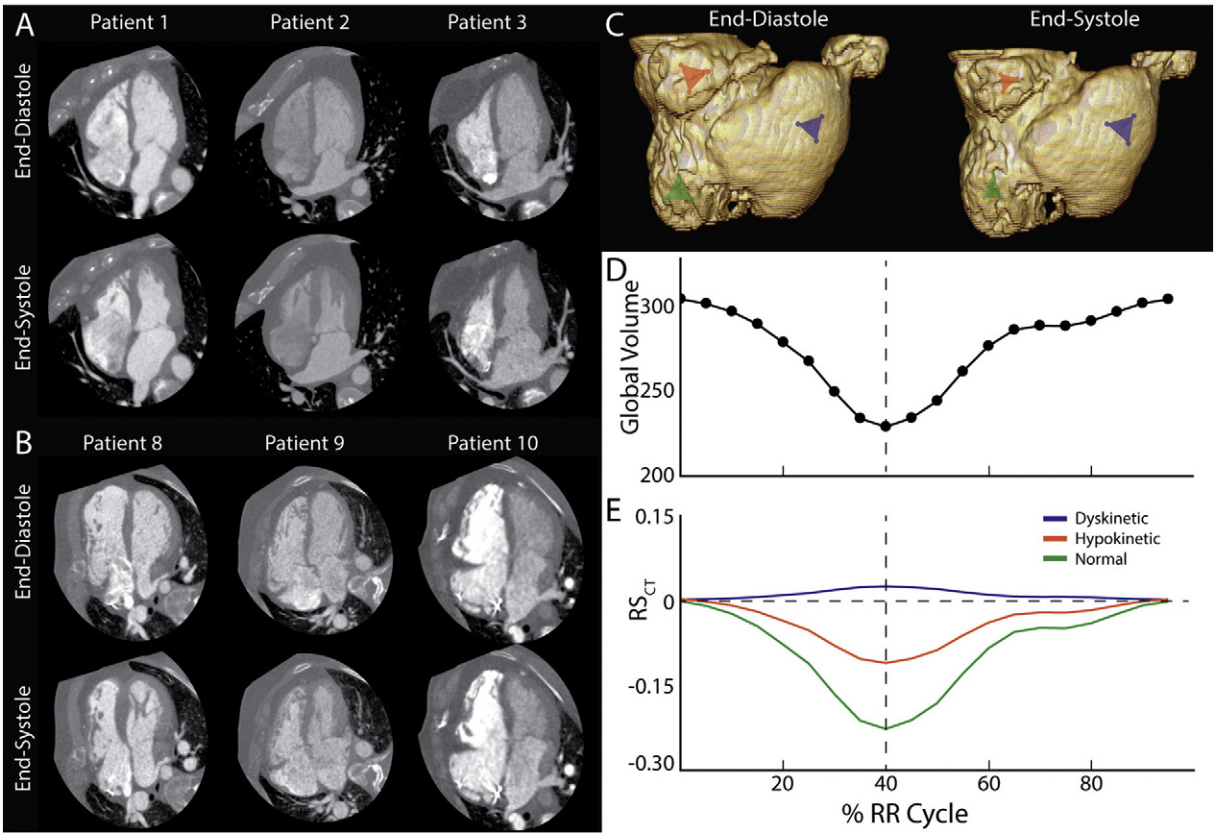

Fig. 1. A) End-diastolic and end-systolic four-chamber images of 3 non-congenital patients. WL/WW: 200/2000. B) End-diastolic and end-systolic four-chamber images of 3 ACHD patients (8–10) with Tetralogy of Fallot. WL/WW: 200/2000. C–E) Quantification of regional shortening. SQUEEZ analysis provides estimates of regional deformation of small triangular patches along the endocardial surface. The size of the patches have been exaggerated for visualization in panel C. Three exemplary regions showing normal contraction (green), hypokinesia (orange), and dyskinesia (blue) are shown. The global volume curve (panel D) is used to estimate end-systole. This point is used to identify end-systolic regionals shortening values from the time curves in panel E.

3.2. Imaging radiation dose and RV contrast enhancement

The radiation dose and RV myocardium – blood contrast for all patients are shown in Table 1. The radiation doses were comparable ($p = 0.37$) but the ACHD patients had images with higher contrast ($p < 0.01$) and CNR ($p = 0.04$). This can be attributed to imaging being timed earlier to ensure RV enhancement and a lower tube potential in some of the ACHD patients compared to imaging of non-congenital patients which targeted enhancement of the left ventricle and coronary arteries.

End-diastolic and end-systolic images for 3 non-congenital patients and 3 ACHD patients are shown in Fig. 1A and B. Biventricular function is displayed via conventional echocardiographic views in Supplementary Movies 1 and 3.

3.3. Global function quantification

Segmentation of the right ventricle throughout the cardiac cycle allowed for volumetric quantification, measurement of end-diastolic and end-systolic volume, stroke volume, and estimation of ejection

Table 2
Global and regional measures of RV function. EDV: end-diastolic volume, ESV: end-systolic volume, SV: stroke volume, EF: ejection fraction, RS_{CT}: mean end-systolic regional shortening, Dyskinesia: percentage of the RV with end-systolic $RS_{CT} > 0$.

Patient	ACHD	EDV (mL)	ESV (mL)	SV (mL)	EF (%)	RS_{CT}	Dyskinesia (%)
1	N	112.3	52.6	59.7	51.4	−0.17 ± 0.07	0.3
2	N	185.9	99.6	86.3	45.2	−0.15 ± 0.08	4.7
3	N	139.4	78.6	60.7	43.6	−0.12 ± 0.09	2.3
4	N	104.4	66.8	37.7	36.1	−0.15 ± 0.14	7.7
5	N	76.4	43.9	32.5	42.6	−0.17 ± 0.05	0.4
6	N	121.0	70.0	51.0	42.2	−0.14 ± 0.08	3.0
7	N	121.5	56.0	65.5	53.9	−0.19 ± 0.06	0.0
		123.0 ± 33.8	66.8 ± 18.6	56.2 ± 18.1	45.0 ± 6.0	−0.16 ± 0.02	2.6 ± 2.8
8	Y	364.1	247.3	116.8	32.1	−0.13 ± 0.10	12.8
9	Y	399.6	252.2	147.4	31.1	−0.03 ± 0.19	9.9
10	Y	321.6	230.2	91.4	24.1	−0.07 ± 0.08	11.9
11	Y	406.7	286.1	120.6	27.4	−0.09 ± 0.08	16.5
12	Y	121.7	76.1	45.6	36.8	−0.13 ± 0.11	11.2
13	Y	256.6	148.2	108.4	36.1	−0.12 ± 0.07	4.5
14	Y	206.1	131.5	74.6	36.2	−0.12 ± 0.09	9.4
		296.6 ± 106.7	195.9 ± 77.4	100.7 ± 33.4	32.0 ± 4.9	−0.10 ± 0.04	10.9 ± 3.7

fraction. The results are shown in Table 2. Volume over time curves for patient 1 and patient 8 are shown in Fig. 2A–B.

The right ventricles of the ACHD patients were larger ($p = 0.001$), had higher end-systolic ($p = 0.001$) and stroke volumes ($p = 0.009$), and had lower global function ($p = 0.001$) compared to the non-congenital controls.

3.4. Regional assessment of function

Regional shortening was measured in all patients throughout the RV endocardial surface. Four views of the end-systolic shortening are shown in Fig. 2C and D for patient 1 (non-congenital) and 8 (ACHD), respectively. 360 degree rotations of the end-systolic shortening are available in Supplementary Movies 2 and 4. The distribution of end-systolic regional shortening values are shown in Fig. 2E and F. The dyskinetic fraction of the RV endocardial surface ($RS_{CT} > 0$ at end-systole) was quantified and is reported in Table 2. Congenital patients demonstrated both lower average RS_{CT} across the RV ($p = 0.003$) as well as increased dyskinetic endocardial area ($p < 0.001$).

4. Discussion

In this pilot study, we demonstrated that four-dimensional estimation of global and regional right ventricular systolic function with cine cardiac CT can be obtained in patients with complex ventricular geometry, including those with congenital heart disease and implanted metal such as pacemakers and defibrillators. In our study, we observed the expected global RV dilation and reduced ejection fraction in the Tetralogy of Fallot patients. In addition, we were able to perform regional shortening analysis which demonstrated large regions of right ventricular dyskinesia in the Tetralogy of Fallot patients relative to the non-congenital controls. While the extent of the dyskinetic regions varied between the individual patients, they were primarily located within the right ventricular outflow tract related to the transannular patch.

Despite global RV dilation, decreased ejection fraction, and regions of dyskinesia, we observed regions with preserved shortening in the Tetralogy of Fallot patients (Fig. 2D). This suggests our method can identify not only the regions of dyskinesia but also regions of preserved functional myocardium. This regional assessment could provide important

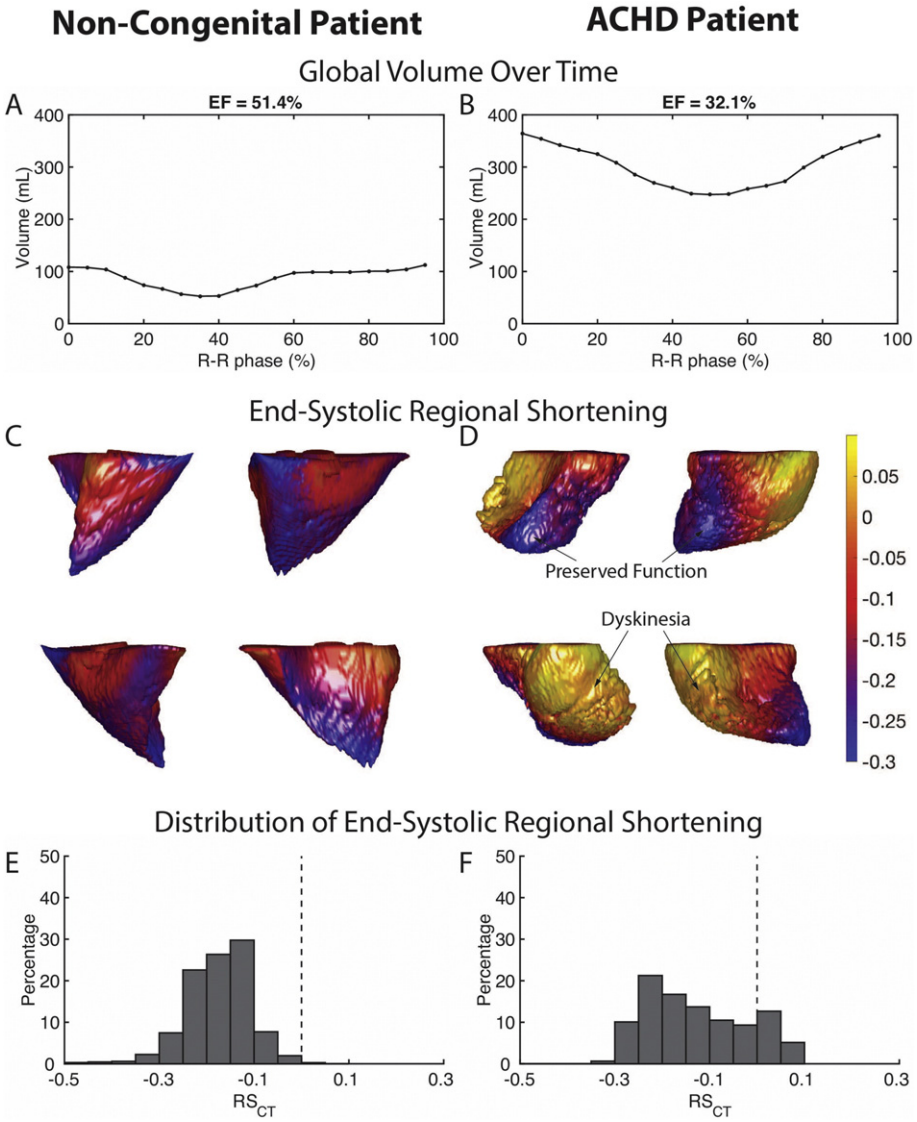

Fig. 2. Global and regional quantification of non-congenital and ACHD patient. Global RV function measured from the change in blood pool volume for patient 1 (panel A) and patient 8 (panel B) illustrate the extent of dilation in an ACHD patient. Four views of the regional shortening at end-systole are shown for patient 1 (panel C) and patient 8 (panel D). The areas of dyskinesia (end-systolic dilation, shown in yellow) occur along the anterior free wall and outflow tract. Histogram analysis (panel E and F) illustrates the distribution of regional shortening, limitations with measurement of an average value, and the percentage of RV endocardium that is dyskinetic.

information for early detection of dysfunction, treatment planning, and treatment response beyond what is observed from global measures such as end-diastolic volume or ejection fraction.

Recent work has shown that cardiac MRI measurements of global left and right ventricular systolic function can improve risk stratification for ventricular arrhythmias and death in adult Tetralogy of Fallot patients [9]. These risk models may identify those high-risk Tetralogy of Fallot patients who would benefit from an implantable cardioverter-defibrillator [9–11]. The method described in this report provides these global measurements as well as regional measures of systolic function and is not contraindicated in patients with pacemaker or defibrillators. Future research is needed to assess whether the quantity of dyskinetic segments is a marker for increased risk for future ventricular failure or ventricular arrhythmias.

In our study, four of the 7 ACHD patients had contraindications for MRI due to implanted metal (pacemaker, defibrillator, and breast tissue expander). With decreasing radiation doses and a population increasingly requiring pacemaker or defibrillator implantation, cardiac CT may become more widely used in the ACHD population [4,12]. The presence of cardiac devices did not limit the ability of our approach with cardiac CT to provide global or regional quantification. As a result, our approach of low radiation dose CT imaging combined with global and regional quantification of systolic function has the potential to enable longitudinal assessment of patients including pre- and post-surgical intervention.

Our study incorporated two distinct populations which required very different scanning parameters: one without congenital heart disease being evaluated for coronary artery disease and one with congenital heart disease being evaluated for ventricular shape and function. For the assessment of coronary artery disease, higher resolution imaging requires higher tube currents for improved image quality to visualize sub-millimeter stenoses and coronary plaques. For adult congenital heart disease, the clinical assessment of cardiac size and function is obtained with lower radiation dose technique with low mA and low kVp techniques to minimize radiation exposure. Nevertheless, the SQUEEZ algorithm for quantification of regional function was able to provide robust results over a wide variety of tube currents in these two populations.

Our mean radiation dose in ACHD patients (2.1 mSv) was higher than the 0.94 mSv median dose previously reported [4]. This was due to two several factors. First, patients had higher BMIs ($28.1 \pm 4.2\ kg/m^2$) than the prior study cohort ($24.2 \pm 4.3\ kg/m^2$). Furthermore, patient 8 and 12 had arrhythmias during imaging which led to multiple heart beat acquisition and further increased the radiation dose. Finally, 3 of the 7 ACHD patients were referred for assessment of biventricular function as well as coronary artery evaluation. This led to utilizing dose modulation with increased mA at end-diastole for appropriate visualization of the coronary arteries, which also contributed to the increased radiation dose.

4.1. Limitations

This work is a pilot study with retrospective analysis of fourteen patients. The CT-derived measures of systolic function were not validated against a gold standard. Most of the ACHD patients in our study had contraindications to MRI and the remaining ACHD patients and normal controls were referred for non-invasive assessment of coronary artery disease. Due to the retrospective design, neither MRIs nor volumetric echocardiography were obtained in these subjects. However, previous work has shown close agreement between CT and MR-derived measures of function in ACHD patients. Yamasaki et al. demonstrated high correlation between RV measures ($r = 0.71–0.96$), slight overestimation of RV EDV (17.1 mL), ESV (12.9 mL), and SV (4.2 mL), slight underestimation of RV EF (2.6%), and lower variability in CT-derived measures relative to MRI [7].

The study utilized a 320-detector row CT scanner which is available at a limited number of centers. Although the quantification could be performed on scans obtained with fewer detector rows, it could introduce stitching artifacts and result in higher radiation dose.

5. Conclusions

In this initial pilot study, global and regional systolic function were successfully measured using low radiation dose 4D cine CT with SQUEEZ quantification in non-congenital patients as well as ACHD patients with Tetralogy of Fallot.

Supplementary data to this article can be found online at http://dx.doi.org/10.1016/j.ijcard.2017.08.040.

Funding sources

This work was supported by the National Institutes of Health (grant number 1ZIAHL006138-05 and K12GM068524), University of California President's Postdoctoral Fellowship, and UC San Diego Frontiers of Innovation Scholar Program.

Conflicts of interest

The National Heart, Lung, and Blood Institute of the National Institutes of Health has an institutional research agreement with Toshiba Medical Systems.

Acknowledgments

None.

References

[1] D. Van Der Linde, E.E.M. Konings, M.A. Slager, M. Witsenburg, W.A. Helbing, J.J.M. Takkenberg, J.W. Roos-Hesselink, Birth prevalence of congenital heart disease worldwide: a systematic review and meta-analysis, J. Am. Coll. Cardiol. 58 (2011) 2241–2247.

[2] W. Budts, J. Roos-Hesselink, T. Rädle-Hurst, A. Eicken, T.A. McDonagh, E. Lambrinou, M.G. Crespo-Leiro, F. Walker, A.A. Frogoudaki, Treatment of heart failure in adult congenital heart disease: a position paper of the Working Group of Grown-Up Congenital Heart Disease and the Heart Failure Association of the European Society of Cardiology, Eur. Heart J. 37 (2016) 1419–1427.

[3] A.M. Valente, S. Cook, P. Festa, H.H. Ko, R. Krishnamurthy, A.M. Taylor, C.A. Warnes, J. Kreutzer, T. Geva, Multimodality imaging guidelines for patients with repaired tetralogy of Fallot: a report from the American Society of Echocardiography, J. Am. Soc. Echocardiogr. 27 (2014) 111–141.

[4] D.W. Groves, L.J. Olivieri, S.M. Shanbhag, K.C. Bronson, J.H. Yu, E.A. Nelson, S.F. Rollison, M.S. Stagliano, A.S. John, K. Kuehl, M.Y. Chen, Feasibility of low radiation dose retrospectively-gated cardiac CT for functional analysis in adult congenital heart disease, Int. J. Cardiol. 228 (2017) 180–183.

[5] A. Pourmorteza, K.H. Schuleri, D.A. Herzka, A.C. Lardo, E.R. McVeigh, A new method for cardiac computed tomography regional function assessment: stretch quantifier for endocardial engraved zones (SQUEEZ), Circ. Cardiovasc. Imaging 5 (2012) 243–250.

[6] A. Pourmorteza, M.Y. Chen, J. Pals, A.E. Arai, E.R. Mcveigh, Correlation of CT-based regional cardiac function (SQUEEZ) with myocardial strain calculated from tagged MRI: an experimental study, Int. J. Card. Imaging 32 (2016) 817–823.

[7] Y. Yamasaki, M. Nagao, K. Yamamura, M. Yonezawa, Y. Matsuo, S. Kawanami, T. Kamitani, K. Higuchi, I. Sakamoto, Y. Shiokawa, H. Yabuuchi, H. Honda, Quantitative assessment of right ventricular function and pulmonary regurgitation in surgically repaired tetralogy of Fallot using 256-slice CT: comparison with 3-Tesla MRI, Eur. Radiol. 24 (2014) 3289–3299.

[8] A.J. Van der Molen, R.M.S. Joemai, J. Geleijns, Performance of longitudinal and volumetric tube current modulation in a 64-slice CT with different choices of acquisition and reconstruction parameters, Phys. Med. 28 (2012) 319–326.

[9] J.P. Bokma, K.C. de Wilde, H.W. Vliegen, A.P. van Dijk, J.P. van Melle, F.J. Meijboom, A.H. Zwinderman, M. Groenink, B.J.M. Mulder, B.J. Bouma, Value of cardiovascular magnetic resonance imaging in noninvasive risk stratification in tetralogy of Fallot, JAMA Cardiol. (2017) 1–6.

[10] P. Khairy, S.M. Fernandes, J.E. Mayer, J.K. Triedman, E.P. Walsh, J.E. Lock, M.J. Landzberg, Long-term survival, modes of death, and predictors of mortality in patients with Fontan surgery, Circulation 117 (2008) 85–92.

[11] P. Khairy, G.F. van Hare, S. Balaji, C.I. Berul, F. Cecchin, M.I. Cohen, C.J. Daniels, B.J. Deal, J.A. Dearani, N. de Groot, A.M. Dubin, L. Harris, J. Janousek, R.J. Kanter, P.P. Karpawich, J.C. Perry, S.P. Seslar, M.J. Shah, M.J. Silka, J.K.

Triedman, E.P. Walsh, C.A. Warnes, PACES/HRS expert consensus statement on the recognition and management of arrhythmias in adult congenital heart disease, Can. J. Cardiol. 30 (2014) e1–e63.

[12] A.R. Opotowsky, O.K. Siddiqi, G.D. Webb, Trends in hospitalizations for adults with congenital heart disease in the U.S. J. Am. Coll. Cardiol. 54 (2009) 460–467.